Title
COHERENT AVERAGING OF ELECTRON SPINS BY ROTARY ECHOES IN EXCITED TRIPLET STATES

Author
Tarrasch, M.E.

Publication Date
1978-09-01

Submitted to CHEMICAL PHYSICS

LBL-7307
Preprint

COHERENT AVERAGING OF ELECTRON SPINS BY ROTARY ECHOES IN EXCITED TRIPLET STATES

M. E. Tarrasch and C. B. Harris

September 1978

Prepared for the U. S. Department of Energy
under Contract W-7405-ENG-48

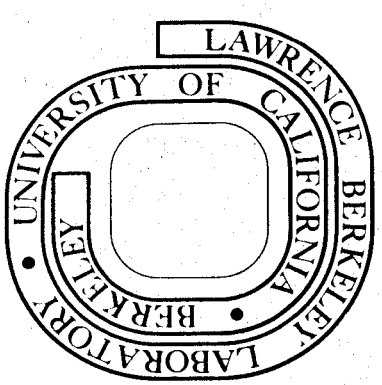

DISCLAIMER

COHERENT AVERAGING OF ELECTRON SPINS BY ROTARY ECHOES IN EXCITED TRIPLET STATES

M. E. Tarrasch and C. B. Harris

Department of Chemistry and
Materials and Molecular Research Division
Lawrence Berkeley Laboratory
University of California
Berkeley, California 94720

ABSTRACT

A theoretical treatment of rotary echoes derived from Average Hamiltonian formalism in photoexcited triplet states is presented. From a general relaxation matrix, it is shown that relaxation fields perpendicular to the driving field $\underset{\sim}{H}_{eff}$ are completely averaged, whereas relaxation fields parallel to $\underset{\sim}{H}_{eff}$ are not. Rotary echoes are found to differ from other coherence techniques only in the geometry of the experiment and not in the averaging properties per se. Off-resonance driving field conditions are shown to impair the efficiency of the averaging and to cause beats in the observed echo decay. Finally, inhomogeneous line broadening is shown to produce a damped echo decay with beats even when the field is on-resonance.

I. INTRODUCTION

The use of spin coherence experiments for studying excited triplet states in molecular solids has been demonstrated many times in the last few years.[1] For these systems, two general features are important: 1) the inhomogeneous broadening of most ESR absorption lines obscures any CW measurements of relaxation processes and necessitates the use of time-resolved spectroscopy; and 2) the *optical detection* of spin coherence requires that the coherent component be manifested as a population term and thus most pulse sequences which coherently saturate the system must include a $\pi/2$ "probe pulse" to rotate the coherent component into a population difference.[2] The exceptions to this are transient nutations, rotary echoes, and rotary echo trains. The purpose of this paper is to present a theoretical investigation of rotary echoes,[3] a relatively simple coherence technique designed to eliminate applied field ($\underset{\sim}{H}_1$) inhomogeneities. In this instance, no probe pulse is required because the echo forms along the r_3 axis in the Feynman-Vernon-Hellwarth (FVH) representation.[4] The rotary echo is a pair of back-to-back transient nutations separated by a 180° phase shift in the applied field and consequently it uses neither a preparation nor a probe pulse. Since the $\underset{\sim}{r}$-vector is continuously "sampling" the r_1-r_2 plane and the r_3 axis, the decay of the echo is characterized by a relaxation time $T_{2\rho}^{-1} = \frac{1}{2}(T_1^{-1} + T_2^{-1}) = (2T_2)^{-1}$ in the absence of spin-lattice relaxation.

In the first section of this paper, we apply Average Hamiltonian theory[5] to the rotary echo. This approach allows a quantitative description of the echo phenomenon to be derived and also allows one to clearly

differentiate the rotary echo from several other coherence experiments. Off-resonance effects are then discussed with respect to the averaging efficiency of the rotary echo. Because the geometrical refocusing of the echo will also be affected by going off-resonance, quantitative expressions for the echo intensity are presented and applied to inhomogeneous absorption lines.

Although this work was motivated by triplet state ESR considerations, we would like to mention the general applicability of these results to other fields. It can be extended to the optical regime when the usual assumption that $\lambda^3 >> V$ (the sample volume) is made.[6] In such cases, spatial effects can be neglected and the equations presented in Section II are valid. Field strengths vary spatially across a laser beam and molecular transition dipoles can have different orientations with respect to the electric field vector; thus, the problem of driving field inhomogeneities is as germane to the optical case as it is to the magnetic case.

II. COHERENT AVERAGING VIA ROTARY ECHOES

In applying Average Hamiltonian formalism to rotary echoes, we will follow the notation and conventions of Breiland, Brenner, and Harris (BBH).[2] The time evolution of a general Hermitian operator $\mathcal{H}$ is determined by the following operator in the z-y-x basis for the triplet state:

$$S = \exp\frac{-i\mathcal{H}t}{\hbar} = \begin{array}{c} \begin{matrix} \quad |z\rangle & \quad\quad |y\rangle & \quad\quad\quad |x\rangle \end{matrix} \\ \begin{bmatrix} e^{(-iE_z\Delta\omega t/\hbar\omega_o)} & 0 & 0 \\ 0 & \frac{-i\Delta\omega}{\bar{\omega}}\sin\frac{\bar{\omega}t}{2} + \cos\frac{\bar{\omega}t}{2} & \frac{\omega_1}{\bar{\omega}}e^{-i\phi}\sin\frac{\bar{\omega}t}{2} \\ 0 & \frac{-\omega_1}{\bar{\omega}}e^{+i\phi}\sin\frac{\bar{\omega}t}{2} & \frac{i\Delta\omega}{\bar{\omega}}\sin\frac{\bar{\omega}t}{2} + \cos\frac{\bar{\omega}t}{2} \end{bmatrix} \end{array} . \tag{1}$$

Here, the $|y\rangle$ and $|x\rangle$ sublevels (energies Y and X, respectively) are being coupled by the microwaves of frequency $\omega_o + \Delta\omega$, $\omega_o = (Y-X)/\hbar$, $E_z = Z - (X + Y)/2$, ω_1 is the applied field strength, $\Delta\omega$ is the amount off-resonance, and $\bar{\omega} = (\omega_1^2 + \Delta\omega^2)^{\frac{1}{2}}$. After a rotation by an angle $\theta = \bar{\omega}t$, the operator $\mathcal{H}(\theta)$ is then given by

$$\mathcal{H}(\theta) = S\mathcal{H}S^{-1} . \tag{2}$$

A. On-Resonance

Identifying $\mathcal{H}$ as a relaxation Hamiltonian $\mathcal{H}_R$ in the rotating frame with all non-zero components H_{ij}, a rotation by angle θ with $\Delta\omega = \phi = 0$ yields

$$\mathcal{H}_R(\theta) = \begin{bmatrix} H_{zz} & \left(H_{zy}\cos\frac{\theta}{2} + H_{zx}\sin\frac{\theta}{2}\right) & \left(H_{zx}\cos\frac{\theta}{2} - H_{zy}\sin\frac{\theta}{2}\right) \\ \left(H_{yz}\cos\frac{\theta}{2} + H_{xz}\sin\frac{\theta}{2}\right) & \begin{matrix} H_{xx}\sin^2\frac{\theta}{2} + H_{yy}\cos^2\frac{\theta}{2} \\ +(H_{xy}+H_{yx})\sin\frac{\theta}{2}\cos\frac{\theta}{2} \end{matrix} & \begin{matrix} H_{yx}\cos^2\frac{\theta}{2} - H_{xy}\sin^2\frac{\theta}{2} \\ -(H_{yy}-H_{xx})\sin\frac{\theta}{2}\cos\frac{\theta}{2} \end{matrix} \\ \left(H_{xz}\cos\frac{\theta}{2} - H_{yz}\sin\frac{\theta}{2}\right) & \begin{matrix} H_{xy}\cos^2\frac{\theta}{2} - H_{yx}\sin^2\frac{\theta}{2} \\ -(H_{yy}-H_{xx})\sin\frac{\theta}{2}\cos\frac{\theta}{2} \end{matrix} & \begin{matrix} H_{yy}\sin^2\frac{\theta}{2} + H_{xx}\cos^2\frac{\theta}{2} \\ -(H_{xy}+H_{yx})\sin\frac{\theta}{2}\cos\frac{\theta}{2} \end{matrix} \end{bmatrix} . \tag{3}$$

When the applied $\underset{\sim}{H}_1$ field is "on" for a time τ and rotates the $\underset{\sim}{r}$-vector through an angle

$$\Theta >> 2\pi \quad , \tag{4}$$

the averaged relaxation matrix $\bar{\mathcal{H}}_R$ can be determined by incrementing the rotation angle by $d\theta$ and assigning a waiting time of $\tau d\theta/\Theta$ to each value of $\mathcal{H}_R(\theta)$. The result in the limit that $d\theta$ approaches zero is:

$$\bar{\mathcal{H}}_R^{0^\circ} = \frac{\sum_{i=1}^{\Theta/d\theta} \mathcal{H}_R(id\theta)}{\tau} \frac{\tau d\theta}{\Theta} \longrightarrow \frac{1}{\Theta}\int_0^{\Theta} \mathcal{H}_R(\theta)d\theta \ . \tag{5}$$

Using the inequality (4) to neglect terms of order $(\sin\theta)/\theta$, $(\sin^2\theta)/\theta$, etc., we obtain for the 0° phase pulse:

$$\bar{\mathcal{H}}_R^{0^\circ} = \frac{1}{2}\begin{bmatrix} 2H_{zz} & 0 & 0 \\ 0 & H_{xx}+H_{yy} & H_{yx}-H_{xy} \\ 0 & H_{xy}-H_{yx} & H_{xx}+H_{yy} \end{bmatrix} . \tag{6}$$

One can then take the matrix $\mathcal{H}_R(\Theta)$ as a zero-time matrix for the 180° pulse and operate on it in the same manner with S and S^{-1}, choosing $\phi = 180°$. $\bar{\mathcal{H}}_R^{180^\circ}$ is identical to $\bar{\mathcal{H}}_R^{0^\circ}$ and therefore $\bar{\mathcal{H}}_R = \frac{1}{2}[\bar{\mathcal{H}}_R^{0^\circ} + \bar{\mathcal{H}}_R^{180^\circ}] = \bar{\mathcal{H}}_R^{0^\circ}$.

The first point that emerges from this treatment is that the second half of the pulse sequence is unnecessary with respect to the averaging of the relaxation Hamiltonian. A transient nutation performs the same averaging as the rotary echo. It cannot, however, eliminate

$\underset{\sim}{H}_1$ inhomogeneities and is therefore of little value for measuring relaxation times relative to the rotary echo decay. It should be pointed out that a rotation by 2π does not return $\mathcal{H}_R$ to its original form due to the spinor properties of a spin-1/2 system. For a triplet state, the true cycle time is $t_c = 4\pi/\omega_1$, even though one loosely speaks of the cycle time as being 2τ, the time it takes for the echo to form.

Looking at Eq. (6), we see that all off-diagonal terms involving the $|z\rangle$ sublevel are averaged to zero as expected. Since this will always be the case when only two of the three sublevels are coupled, we will drop the $|z\rangle$ sublevel column and row from $\mathcal{H}_R$ and work only with 2×2 matrices for the sake of clarity.

The most important thing to note about the 2×2 submatrix in Eq. (6) is that the *diagonal terms are identical*. Physically, this corresponds to adding the *same* energy term, $\frac{1}{2}(H_{xx}+H_{yy})$, to the energy of each sublevel coupled by the microwaves. Assuming that the values of H_{xx} and H_{yy} vary over the different sites in the sample (inhomogeneous broadening), the rotary echo can be seen to eliminate the effects of a distribution of relaxation strengths. Figure 1 illustrates this in more detail. Before the application of the echo, the $|x\rangle \leftrightarrow |y\rangle$ transition would appear at the energy $Y - X + H_{yy} - H_{xx}$. Since the quantity $H_{yy} - H_{xx}$ may vary from site to site, it contributes to the linewidth of the absorption; however, after applying the echo sequence, the absorption now occurs at energy Y-X and the contribution of the relaxation term to the linewidth is removed.

More quantitatively, in the FVH representation,

$$\frac{dr_1}{dt} = -(H_{yy} - H_{xx}) \frac{r_2}{\hbar} - \frac{2}{\hbar} (\text{Im } H_{yx}) r_3 \tag{7a}$$

$$\frac{dr_2}{dt} = -\frac{2}{\hbar} (\text{Re } H_{yx})\, r_3 + (H_{yy} - H_{xx}) \frac{r_1}{\hbar} \tag{7b}$$

$$\frac{dr_3}{dt} = \frac{2}{\hbar} (\text{Re } H_{yx})\, r_2 + \frac{2}{\hbar} (\text{Im } H_{yx}) r_1 \quad . \tag{7c}$$

Thus, the time dependence of the spin polarization r_3 requires that the off-diagonal matrix elements be non-zero in the rotating frame. For triplet states at low temperatures, one usually assumes that $T_1 = \infty$; this corresponds to setting H_{yx} and H_{xy} equal to zero. Since T_2 processes then depend solely on the difference of the diagonal terms $H_{yy} - H_{xx}$, Eqs. (6) and (7) show that r_1 and r_2 are made time-independent by the averaging of $\mathcal{H}_R$.

The directional dependence of the averaging process in the rotating frame can be elucidated by representing the relaxation field as a field $\underset{\sim}{\Omega}^R$ which exerts a torque on $\underset{\sim}{r}$.[4] The components of $\underset{\sim}{\Omega}^R$ are

$$\Omega_1^R = \frac{(H_{xy} + H_{yx})}{\hbar} \tag{8a}$$

$$\Omega_2^R = \frac{i(H_{yx} - H_{xy})}{\hbar} \tag{8b}$$

$$\Omega_3^R = \frac{H_{yy} - H_{xx}}{\hbar} \tag{8c}$$

and the general driving field Hamiltonian for the y-x basis in the rotating frame is

$$\mathcal{H}^* = \frac{\hbar}{2}\begin{bmatrix} \Delta\omega & i\omega_1 e^{-i\phi} \\ -i\omega_1 e^{i\phi} & -\Delta\omega \end{bmatrix} . \qquad (9)$$

For on-resonance, with $\phi = 0$,

$$\Omega_1^* = 0 \qquad (10a)$$

$$\Omega_2^* = -\omega_1 \qquad (10b)$$

$$\Omega_3^* = 0 \qquad (10c)$$

and the field is applied along the r_2 axis as expected. From the 2×2 submatrix in Eq. (6), the relaxation fields are:

$$\bar{\Omega}_1^R = 0 \qquad (11a)$$

$$\bar{\Omega}_2^R = \frac{i}{\hbar}(H_{yx} - H_{xy}) = -\frac{2}{\hbar}\,\mathrm{Im}\,H_{yx} \qquad (11b)$$

$$\bar{\Omega}_3^R = 0 \quad . \qquad (11c)$$

It is clear that $\underset{\sim}{\bar{\Omega}}^R$ is parallel to $\underset{\sim}{\Omega}^*$ and that the only component of $\underset{\sim}{\Omega}^R$ that is *not* averaged to zero lies along the driving field. The result is that any relaxation field $\underset{\sim}{\Omega}^{R'}$ with $\Omega_1^{R'} = \Omega_2^{R'} = 0$, $\Omega_3^{R'} \neq 0$ before averaging is perpendicular to $\underset{\sim}{\Omega}^*$ and after averaging has all zero components.

One can easily demonstrate that for an arbitrary phase ϕ for the applied field, the argument is identical and no additional insight is gained. The off-resonance case is more important and will be discussed in Section II.B. Thus, *the second general feature of rotary echoes which emerges from this treatment is that all fields perpendicular to*

driving field are averaged but those parallel to it are not.

This analysis allows one to make an interesting comparison between rotary echoes and spin locking. $\bar{\mathcal{H}}_R$ has been calculated by BBH[2] for spin locking and for Carr-Purcell-Meiboom-Gill (CPMG)[7] echo sequences. In both cases, the form of $\bar{\mathcal{H}}_R$ is identical to Eq. (6). How these experiments differ must therefore lie in the geometrical relations between $\underset{\sim}{\Omega}^*$, $\underset{\sim}{\Omega}^R$ and $\underset{\sim}{r}$ itself.

Spin locking is very similar to a rotary echo because the $\underset{\sim}{H}_1$ field is "on" continuously during the course of the experiment. Despite this, the decay of phase coherence as measured by spin locking[8] (called $T_{1\rho}$) has been shown to approach the lifetime of the excited triplet state, whereas phase coherence as measured by rotary echoes is three orders of magnitude shorter. The difference arises because $\underset{\sim}{r}$ lies *along* $\underset{\sim}{\Omega}^*$ in spin locking but is *perpendicular* to it in a rotary echo. If a relaxation field $\underset{\sim}{\Omega}^R$ is present, the only non-zero component of $\bar{\underset{\sim}{\Omega}}^R$ lies along $\underset{\sim}{\Omega}^*$; $\underset{\sim}{r}$ will then precess about the combined field $(\bar{\underset{\sim}{\Omega}}^R + \underset{\sim}{\Omega}^*)$. The presence of the additional field $\bar{\underset{\sim}{\Omega}}^R$ does not affect spin locking, since $\underset{\sim}{r}$ is "locked" along $(\bar{\underset{\sim}{\Omega}}^R + \underset{\sim}{\Omega}^*)$ -- the only difference to be expected is that the rate of relaxation against the fields $(T_{1\rho m}^{-1})$[9] would change, depending on the magnitude of $\bar{\Omega}^R$. Experiments show that $T_{1\rho m}$ processes are slower than most other processes and do not affect the $T_{1\rho}$ value very strongly; any small change in the $T_{1\rho m}$ value is therefore *not* reflected in the $T_{1\rho}$ decay for spin locking.

A rotary echo, however, is much more sensitive to the addition of a small relaxation field $\bar{\underset{\sim}{\Omega}}^R$ along $\underset{\sim}{\Omega}^*$ since $\underset{\sim}{r}$ and $\underset{\sim}{\Omega}^*$ are perpendicular to each other. The rate of precession about $(\bar{\underset{\sim}{\Omega}}^R + \underset{\sim}{\Omega}^*)$ will depend on $|\bar{\underset{\sim}{\Omega}}^R|$.

For a 0°-phase field, the effective field looks like $(\bar{\underset{\sim}{\Omega}}^R + \underset{\sim}{\Omega}^*)$ and for a 180°-phase field, it is $(\bar{\underset{\sim}{\Omega}}^R - \underset{\sim}{\Omega}^*)$; thus, instead of experiencing equal but opposite fields during the echo, there is a refocusing error of $\theta = 4\tau|\bar{\underset{\sim}{\Omega}}^R|$ radians accumulated during the experiment. The echo intensity will decrease by the factor $\cos\theta$, the projection of $\underset{\sim}{r}$ along the r_3 axis at the echo time 2τ. *This, we believe, is an important cause of short* $T'_{2\rho}$ *times in rotary echoes relative to* $T_{1\rho}$ *times in spin locking.* Given that $\bar{\mathcal{H}}_R$ is the same for both spin locking and rotary echoes, but that $T_{1\rho} >> T_{2\rho}$, the above geometrical interpretation is consistent with Redfield's argument that the component of $\underset{\sim}{r}$ parallel to $\underset{\sim}{H}_1$ decays with a time constant T_{2e} (not T_2) in the Bloch equations.[8]

B. Off-Resonance

Off-resonance averaging[10] is considerably more cumbersome to calculate; therefore we will only discuss the 0°-phase field equations for the $|x\rangle \leftrightarrow |y\rangle$ 2×2 submatrix. The averaged Hamiltonian including the 180°-phase field would contain many terms and obscure the physical interpretation.

Neglecting H_{xy} and H_{yx}, the average Hamiltonian for the 0° field is

$$\bar{\mathcal{H}}_R^{0^\circ} = \frac{1}{2}\begin{bmatrix} H_{yy}\left[1+\left(\frac{\Delta\omega}{\bar{\omega}}\right)^2\right] + H_{xx}\left(\frac{\omega_1}{\bar{\omega}}\right)^2 & \frac{i\Delta\omega\omega_1}{\bar{\omega}^2}\left(H_{yy}-H_{xx}\right) \\ \frac{i\Delta\omega\omega_1}{\bar{\omega}^2}\left(H_{xx}-H_{yy}\right) & H_{yy}\left(\frac{\omega_1}{\bar{\omega}}\right)^2 + H_{xx}\left[1+\left(\frac{\Delta\omega}{\bar{\omega}}\right)^2\right] \end{bmatrix}. \tag{12}$$

There are two important differences between this equation and Eq. (6):

1) Even though $\mathcal{K}_R$ was assumed to be diagonal, $\bar{\mathcal{K}}_R$ develops non-zero off-diagonal elements from field-induced T_1 processes. This is strictly an off-resonance effect and can be visualized as follows: the effective field $\underset{\sim}{H}_{eff}$ that $\underset{\sim}{r}$ precesses about lies in the $r_2 - r_3$ plane and $\underset{\sim}{r}$ therefore is not constrained to the $r_1 - r_3$ plane as it would be on-resonance. The cone that $\underset{\sim}{r}$ describes about $\underset{\sim}{H}_{eff}$ leaves $\underset{\sim}{r}$ with a different average projection along the r_3 axis than it would have if $\Delta\omega = 0$. A different r_3 component corresponds to a different spin aligned triplet state and translates mathematically into a non-zero off-diagonal element in $\bar{\mathcal{K}}_R$. Since the number of spins in the system is conserved, this "effective T_1" process must occur simultaneously with an "inverse T_2" process. Indeed, the change in the average r_3 component is accompanied by the creation of a net averaged coherent component along the $\underset{\sim}{H}_1$ direction.

2) The diagonal elements of $\bar{\mathcal{K}}_R^{0°}$ are no longer equal for the off-resonance case. This means that dr_1/dt and dr_2/dt will both depend on the difference of the diagonal terms, which is $(H_{yy} - H_{xx})(\Delta\omega/\bar{\omega})^2$, as well as the real and imaginary parts of the off-diagonal elements. Rewriting Eqs. (7) for off-resonance effects,

$$\frac{dr_1}{dt} = (H_{yy} - H_{xx})\left[-\left(\frac{\Delta\omega}{\bar{\omega}}\right)^2 \frac{r_2}{\hbar} - \left(\frac{\Delta\omega\omega_1}{\bar{\omega}^2}\right) \frac{r_3}{\hbar}\right] \qquad (13a)$$

$$\frac{dr_2}{dt} = (H_{yy} - H_{xx})\left[\left(\frac{\Delta\omega}{\bar{\omega}}\right)^2 \frac{r_1}{\hbar}\right] \qquad (13b)$$

$$\frac{dr_3}{dt} = (H_{yy} - H_{xx})\left[\left(\frac{\Delta\omega\omega_1}{\bar{\omega}^2}\right)\frac{r_1}{\hbar}\right] \quad . \tag{13c}$$

We find for small $\Delta\omega$, terms with the coefficient $\Delta\omega\omega_1/\bar{\omega}^2$ dominate, since $\omega_1 \approx \bar{\omega}$. For large $\Delta\omega$, terms with $(\Delta\omega/\bar{\omega})^2$ are more important. Although it is difficult to estimate the magnitudes of H_{xx} and H_{yy}, a general idea of the effects of off-resonance fields can be obtained if we let $(H_{yy} - H_{xx})$ be five times smaller than the driving field ω_1. In this instance $(H_{yy} - H_{xx})$ is reduced by the factor $\Delta\omega/\bar{\omega}$, that is, the off-resonance averaging increases the dephasing time by about a factor of five. For large $\Delta\omega$, the term $(\Delta\omega/\bar{\omega})^2 \approx 1$ and the averaging is minimal.

One can perhaps gain a clearer physical picture of off-resonance averaging by considering the geometrical components of the relaxation field and the effective field. Again, one finds that any vector perpendicular to $\underset{\sim}{\Omega}^*$ is also perpendicular to $\underset{\sim}{\Omega}^R$ and, as before, fields parallel to the effective field are not averaged while those perpendicular to it are. However, those fields perpendicular to $\underset{\sim}{\Omega}^*$ now lie in a plane, specified by ω_1 and $\Delta\omega$, which does *not* contain the r_3 axis. A relaxation field solely along the r_3 axis, which would be totally averaged were $\Delta\omega = 0$, is now only partially averaged. Referring to Fig. 2, the angle $\underset{\sim}{H}_{eff}$ makes with the r_2 axis is $\alpha = \arctan(\Delta\omega/\omega_1)$. Therefore, any field $\underset{\sim}{\Omega}^R$ along the r_3 axis has a projection $\Omega^R \sin\alpha = \Omega^R(\Delta\omega/\bar{\omega})$ along $\underset{\sim}{H}_{eff}$. *The term $(\Delta\omega/\bar{\omega})$ acts like a reduction factor for the relaxation field strength and physically corresponds to the component of $\underset{\sim}{\Omega}^R$ not averaged (parallel to $\underset{\sim}{H}_{eff}$).* This simple trigonometric argument gives a result very similar to the averaging

treatment, if one assumes that the component of $\underset{\sim}{\Omega}^R$ parallel to $\underset{\sim}{H}_{eff}$ is responsible for relaxation after the application of the echo.

C. Effect of Inhomogeneous Site Distributions

The effects of n-site inhomogeneous broadening in the absence of spin diffusion can be set up using a $2n \times 2n$ block diagonal density matrix for the $\underset{\sim}{r}$-vector components, or equivalently as 3n Bloch equations. It is much simpler to start with an expression for the r_3 component of a *single* $\underset{\sim}{r}$-vector (corresponding to a unique isochromat in the inhomogeneous line) at the echo formation time 2τ. One derives such an expression from the general equations of motion for the components of $\underset{\sim}{r}$:[2]

$$r_1(t) = \frac{1}{\bar{\omega}^2}\left\{r_1(0)\bar{\omega}^2\cos\bar{\omega}t - [r_2(0)\Delta\omega\bar{\omega} + r_3(0)\omega_1\bar{\omega}\cos\phi]\sin\bar{\omega}t + [r_1(0)\omega_1^2\sin^2\phi - r_2(0)\omega_1^2\sin\phi\cos\phi + r_3(0)\omega_1\Delta\omega\sin\phi](1-\cos\bar{\omega}t)\right\} \tag{14a}$$

$$r_2(t) = \frac{1}{\bar{\omega}^2}\left\{r_2(0)\bar{\omega}^2\cos\bar{\omega}t + [r_1(0)\Delta\omega\bar{\omega} - r_3(0)\omega_1\bar{\omega}\sin\phi]\sin\bar{\omega}t + [r_2(0)\omega_1^2\cos^2\phi - r_1(0)\omega_1^2\sin\phi\cos\phi - r_3(0)\omega_1\Delta\omega\cos\phi](1-\cos\bar{\omega}t)\right\} \tag{14b}$$

$$r_3(t) = \frac{1}{\bar{\omega}^2}\left\{r_3(0)\bar{\omega}^2\cos\bar{\omega}t + [r_1(0)\omega_1\bar{\omega}\cos\phi + r_2(0)\omega_1\bar{\omega}\sin\phi]\sin\bar{\omega}t + [r_1(0)\omega_1\Delta\omega\sin\phi - r_2(0)\omega_1\Delta\omega\cos\phi + r_3(0)\Delta\omega^2](1-\cos\bar{\omega}t)\right\}. \tag{14c}$$

These equations describe the time dependence of the $\underset{\sim}{r}$-vector *without* provision for applied field inhomogeneities, relaxation, or triplet state population kinetics.

The calculation of $r_3(2\tau)$ is carried out by first setting $r_1(0) = r_2(0) = \phi \equiv 0$ for the 0°-phase field. The $\underset{\sim}{r}$-vector nutates through an angle $\Theta = \bar{\omega}\tau$ and has all non-zero components at time τ; these components $r_i(\tau)$ now serve as zero-time components for the 180°-phase field, referenced to the starting time τ. Equations (14) are then applied with $\phi = 180°$, again rotating the $\underset{\sim}{r}$-vector through $\Theta = \bar{\omega}\tau$. Since the experimental observable is $r_3(2\tau)$, this is the only component of interest, and is given by

$$r_3(2\tau) = r_3(0)\left(\frac{1}{\bar{\omega}^4}\right)\left[\Delta\omega^2(\Delta\omega^2 - \omega_1^2) + 4\Delta\omega^2\omega_1^2\cos\Theta + \omega_1^2\bar{\omega}^2\sin^2\Theta + (\omega_1^4 - \Delta\omega^2\omega_1^2)\cos^2\Theta\right]. \tag{15}$$

It is important to realize that Eq. (15) describes the intensity of the echo maximum as a function of τ; it does *not* correpond to the echo waveform detected experimentally, but rather to the reduced experimental data after signal intensities have been measured. Calculations based on this equation, with and without population feeding and decay kinetics, are presented in the Appendix of this paper. To simulate inhomogeneous broadening, one numerically integrates across the resonance line, changing $\Delta\omega$ and $r_3(0)$ for each isochromat in the line. The individual values of $r_3(0)$ are weighted appropriately for the chosen lineshape and normalized to $\sum_{i=1}^{n} r_{3_i}(0) = 1.0$. Figures 3 and 4 show the results of such a calculation for both Gaussian and Lorentzian lineshapes. For all of these curves, the resonance line was divided into 251 isochromats extending 5 FWHM's on either side of the center frequency. This rather limited integration range is satisfactory for a Gaussian line, but only gives qualitative results for a Lorentzian. Between five and ten percent of the area

under a Lorentzian line is contained in the wings cut off by the integration, leading to noticeably incorrect normalization for all curves in Fig. 4.

Inhomogeneous broadening shows up as a damping of the echo intensity dependent on the parameters $\Delta\omega$ and $(T_2^*)^{-1} \propto$ FWHM. For a given value of the FWHM, the damping rate increases as $\Delta\omega$ increases and thus the destructive interference of the various $\underset{\sim}{r}$-vectors associated with the isochromats is more efficient as more of the isochromats are off-resonance. The steady state value of $r_3(2\tau)$ is a function of $\Delta\omega$ and reflects the decreasing ability of the field to couple the two levels as $\Delta\omega$ is increased.

The most interesting, and in fact surprising, result of these calculations is demonstrated in Fig. 5, for which the FWHM is varied and the field is applied *on-resonance: the oscillations in* $r_3(2\tau)$ *persist for* $\Delta\omega = 0$ *and are related in frequency and amplitude to the inhomogeneous linewidth* $(T_2^*)^{-1}$. As $(T_2^*)^{-1}$ approaches zero (δ-function line), $r_3(2\tau)$ becomes a flat curve with value 1.0; however, for a typical linewidth experimentally observed, beats in the echo maxima appear. This situation has serious consequences, since these beats are *not* the result of an experimentally determined parameter (i.e., going off-resonance) and are thus unavoidable.

It is extremely difficult to visualize the echo formation in r-space for an inhomogeneous line. Physically, the beats are a consequence of two features: 1) even though $\Delta\omega = 0$, all of the spins are off-resonance by an amount depending on their position in the line; and 2) the applied field is "on" continuously during the experiment and one *cannot* make the approximation used for short pulses ($\theta = \pi/2, \pi$) that all the isochromats

nutate through θ about the same effective field. Because of these characteristics, the rotary echo is the only cyclic coherence experiment which exhibits these beats for on-resonance driving fields.

The observation of these beats would be obscured by experimental error for narrow (FWHM $\lesssim$ 1 MHz) lines; wide lines would also be free of beats if τ were long enough for the oscillations to be damped. For example, in Fig. 5, beats in the decay of the 15 MHz-wide line have nearly disappeared by 2τ = 8 μs. Successful exponential echo decays in molecular crystals have been reported by van't Hof and Schmidt[11] for various Parabenzoquinone (PBQ) systems. The $|z\rangle \leftrightarrow |y\rangle$ transition used to produce the echoes is roughly 15-20 MHz wide in PBQ; thus, it is conceivable that the beats were not observed because τ was chosen long enough to measure the detrapping rates ($10^4 - 10^5$ sec^{-1} in PBQ). For other systems with narrower lines (1 to 5 MHz), these beats persist for much larger values of τ and should be superimposed on the decay due to other processes of interest such as nuclear spin diffusion and trap-exciton band interactions.

ACKNOWLEDGMENTS

The authors are very grateful to H.C. Brenner and A. Pines for many stimulating conversations.

This work was supported by the Division of Chemical Sciences, Office of Basic Energy Sciences, U.S. Department of Energy.

APPENDIX

We present here calculations for rotary echo decays based on the assumption that the resonance line is homogeneous. Although this does not necessarily correspond to the case for ESR absorption lines in solids, the physics is interesting and simpler to visualize than for the case of inhomogeneous broadening.

The results for a single isochromat are described by Eq. (15) and illustrated in Fig. 6. Note that no damping is present as in the case of inhomogeneous broadening and that $\Delta\omega$ alone determines the amplitude and frequency of the oscillations. The frequency increases with increasing $\Delta\omega$, because the $\underset{\sim}{r}$-vector nutates about $\underset{\sim}{H}_{eff}$ with frequency proportional to $\bar{\omega} = \sqrt{\Delta\omega^2 + \omega_1^2}$. The amplitude is a function of the angle α in Fig. 2 and is generally given by $r_3(0)[8\cos^2\alpha - 8\cos^4\alpha]$. When $\alpha = \pi/4$, the resonance offset is equal to the applied field strength and complete inversion can result if τ is such that the phase shift occurs when $\underset{\sim}{r}$ lies along the r_2 axis. Damping due to inhomogeneous broadening would prevent inversion from occurring in most experimental situations.

We will now account for population being fed into the lowest triplet state from the singlet manifold and subsequently decaying to the ground state or other excited states. The time dependence of the density matrix must be modified to include terms which both populate and deplete the diagonal elements at rates F_y, F_x, and k_y, k_x respectively, and terms which deplete the off-diagonal elements at an average rate $k_A = 1/2(k_y + k_x)$. Solutions similar to Eqs. (14) have been presented by Breiland, Fayer, and Harris[6] and can be used to generate an expression for $r_3(2\tau)$ analogous

to Eq. (15). The feeding rates are not variables in this calculation, but are fixed by k_A and $r_3(0)$, which has been set equal to 1.0 to provide comparison with Figs. 3 through 6.

Generally, triplet state lifetimes will not affect echo decays because other processes of interest occur on a much more rapid time scale. The curve for $k_A = 10^2$ sec^{-1} in Fig. 7 represents a typical triplet state lifetime and is virtually identical to the curve in Fig. 6 for $\Delta\omega = 1$ MHz. More rapid decay processes, such as detrapping to a vibronic level,[11] are represented by curves with $k_A \sim 10^5$ to 10^6 sec^{-1} in Fig. 7. Damping is evident and does *not* lead to a steady state $r_3(2\tau)$ value of zero, as would be observed if Eq. (15) were simply convoluted with an exponential decay term. This is because feeding events replenish the cone that $\underset{\sim}{r}$ describes about $\underset{\sim}{H}_{eff}$. Purely homogeneous broadening (decay without feeding) would result in $r_3(2\tau)$ approaching zero but is not observed in molecular solids.

REFERENCES

1. C. B. Harris and W. G. Breiland, "Coherent Spectroscopy in Excited States," Laser and Coherence Spectroscopy, ed. J. I. Steinfeld (Plenum Publishing, New York, 1978).
2. W. G. Breiland, H. C. Brenner, and C. B. Harris, J. Chem. Phys. 62, 3458 (1975); W. G. Breiland, C. B. Harris, and A. Pines, Phys. Rev. Lett. 30, 158 (1973).
3. I. Solomon, Phys. Rev. Lett. 2, 301 (1959); C. B. Harris, R. L. Schlupp, and H. Schuch, Phys. Rev. Lett. 30, 1019 (1973).
4. R. P. Feynman, F. L. Vernon, Jr., and R. W. Hellwarth, J. Appl. Phys. 28, 49 (1957).
5. J. S. Waugh, C. H. Wang, L. M. Huber, and R. L. Vold, J. Chem. Phys. 48, 662 (1968); U. Haeberlen and J. S. Waugh, Phys. Rev. 175, 453 (1968).
6. W. G. Breiland, M. D. Fayer, and C. B. Harris, Phys. Rev. A13, 383 (1976).
7. H. Y. Carr and E. M. Purcell, Phys. Rev. 94, 630 (1954); S. Meiboom and D. Gill, Rev. Sci. Instr. 29, 688 (1958).
8. A. G. Redfield, Phys. Rev. 98, 1787 (1955).
9. M. D. Fayer and C. B. Harris, Chem. Phys. Lett. 25, 149 (1974).
10. U. Haeberlen, J. D. Ellett, Jr., and J. S. Waugh, J. Chem. Phys. 55, 53 (1971); A. Pines and J. S. Waugh, J. Mag. Res. 8, 354 (1972).
11. C. A. van't Hof and J. Schmidt, Chem. Phys. Lett. 36, 457 (1975); Chem. Phys. Lett. 42, 73 (1976).

FIGURE CAPTIONS

Fig. 1. Schematic representation of coherent averaging by rotary echoes.

Fig. 2. Definition of angle α = arctan $(\Delta\omega/\omega_1)$.

Fig. 3. Off-resonance rotary echo decays for a Gaussian line (FWHM= 3 MHz). The driving field strength ω_1 is 5 MHz. The echo signal intensity $r_3(2\tau)$ is plotted as a function of the echo time 2τ for various values of $\Delta\omega$.

Fig. 4. Off-resonance rotary echo decays for a Lorentzian line with FWHM= 3 MHZ (ω_1 = 5 MHz).

Fig. 5. On-resonance rotary echo decays for a Gaussian line as a function of the linewidth (ω_1 = 5 MHz).

Fig. 6. Off-resonance rotary echo decays for a single isochromat (ω_1 = 5 MHz).

Fig. 7. Off-resonance rotary echo decays for a single isochromat including sublevel population kinetics (ω_1 = 5 MHz).

COHERENT AVERAGING *VIA* ROTARY ECHOES

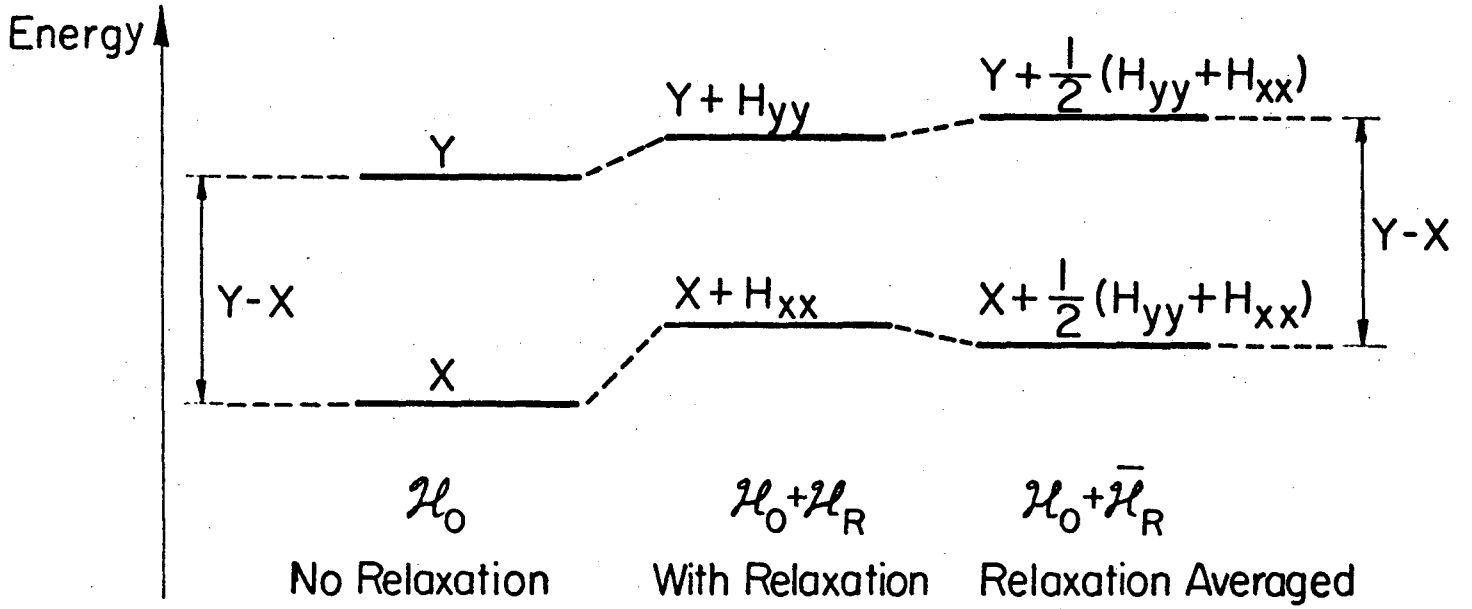

XBL 7711-6492

Figure 1

EFFECTIVE FIELD ORIENTATION FOR OFF-RESONANCE APPLIED FIELD IN ROTATING FRAME

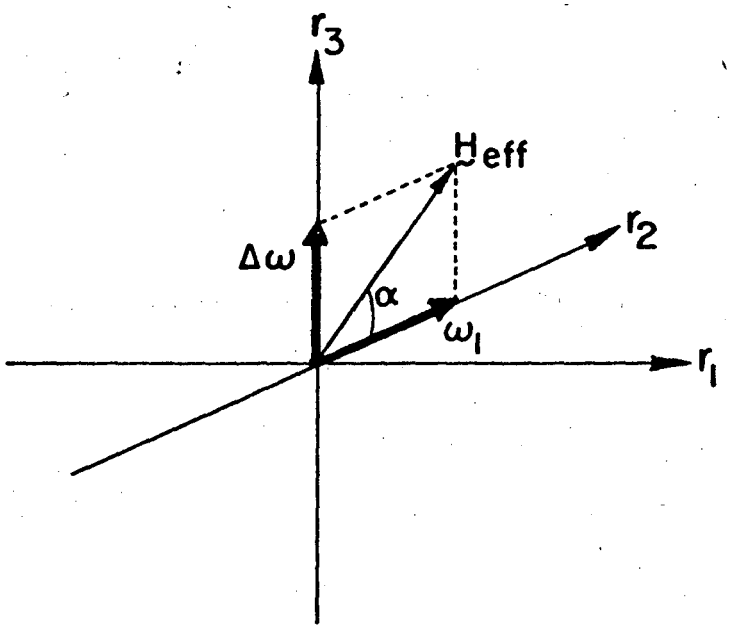

XBL 7711-6490

Figure 2

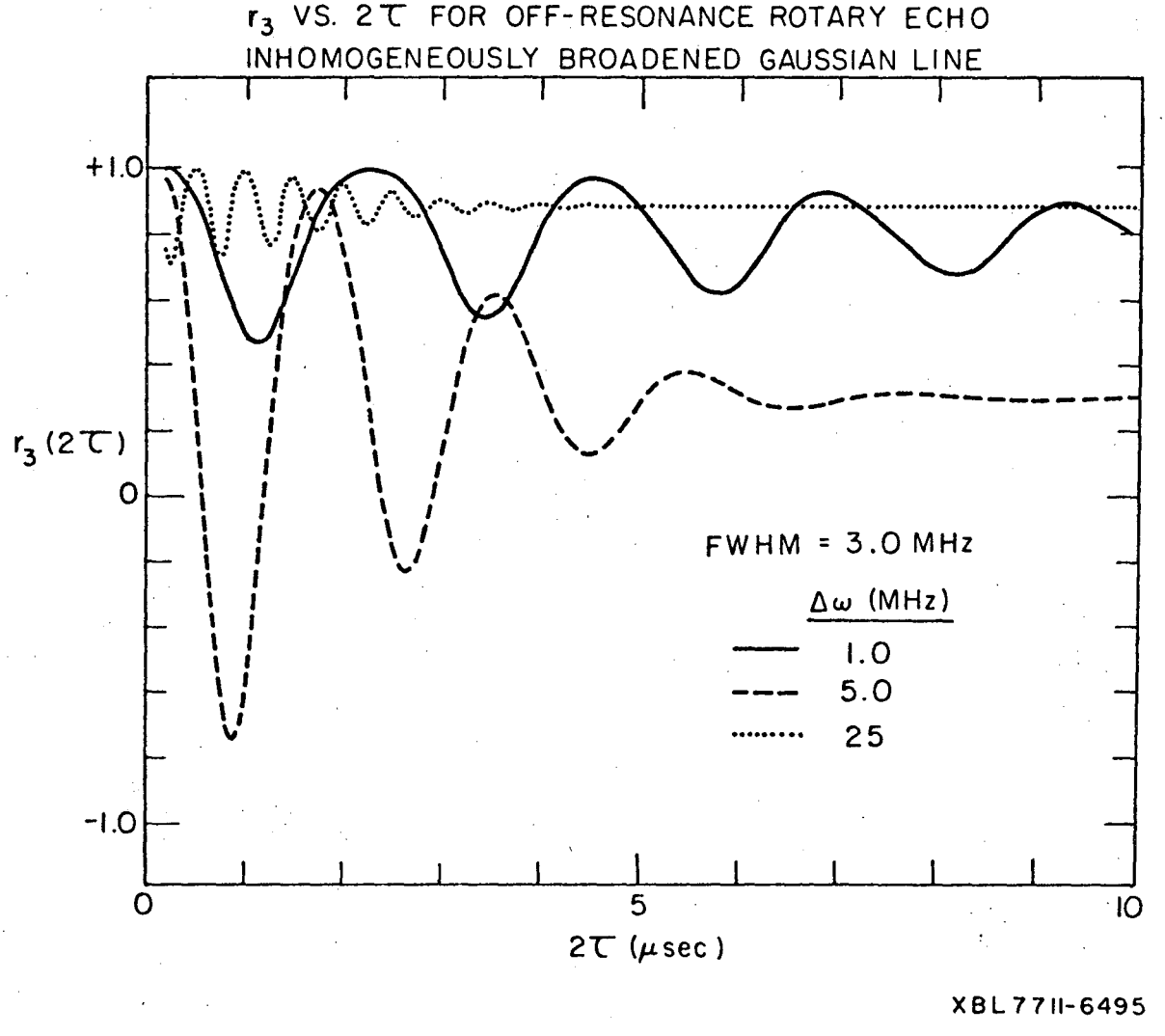
r_3 VS. 2τ FOR OFF-RESONANCE ROTARY ECHO
INHOMOGENEOUSLY BROADENED GAUSSIAN LINE
+1.0
$r_3(2\tau)$
0
-1.0
FWHM = 3.0 MHz
Δω (MHz)
1.0
5.0
25
0
5
10
2τ (μsec)
XBL7711-6495

Figure 3

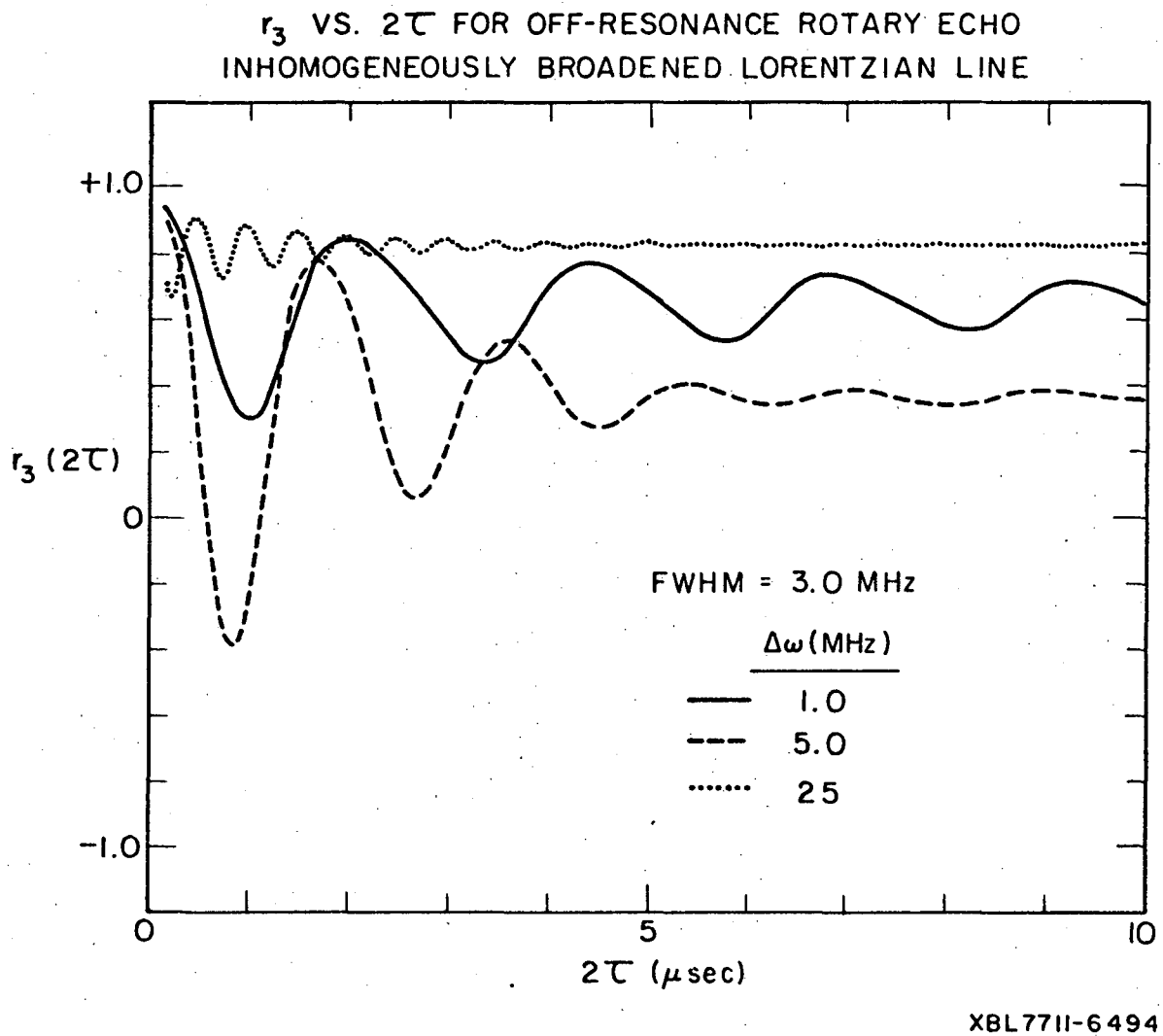
r_3 VS. 2τ FOR OFF-RESONANCE ROTARY ECHO
INHOMOGENEOUSLY BROADENED LORENTZIAN LINE
+1.0
0
-1.0
$r_3(2\tau)$
FWHM = 3.0 MHz
Δω(MHz)
1.0
5.0
25
0
5
10
2τ (μsec)
XBL7711-6494

Figure 4

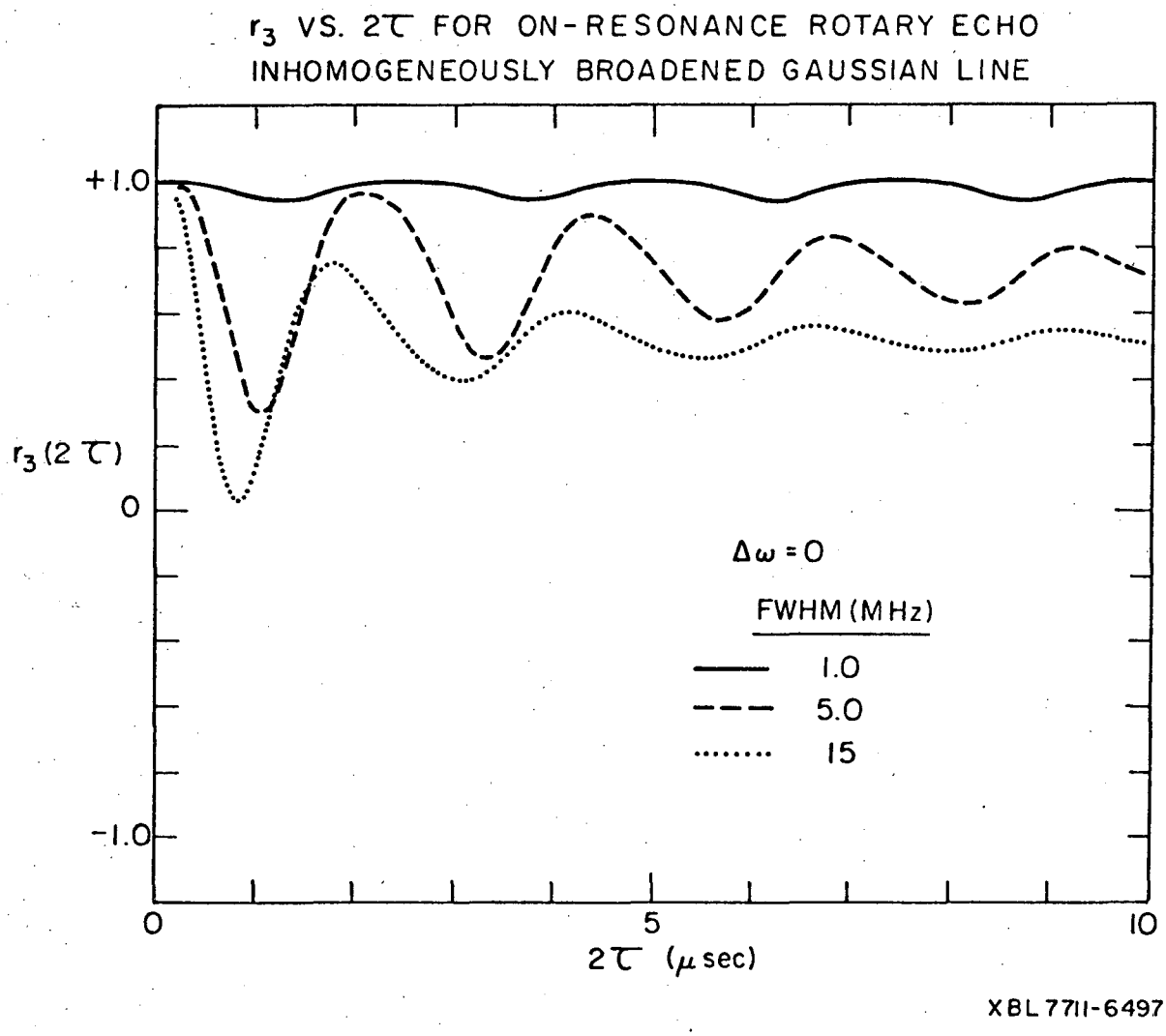
r_3 VS. 2τ FOR ON-RESONANCE ROTARY ECHO
INHOMOGENEOUSLY BROADENED GAUSSIAN LINE
+1.0
$r_3(2\tau)$
0
-1.0
$\Delta\omega = 0$
FWHM (MHz)
1.0
5.0
15
0
5
10
2τ (μsec)
XBL 7711-6497

Figure 5

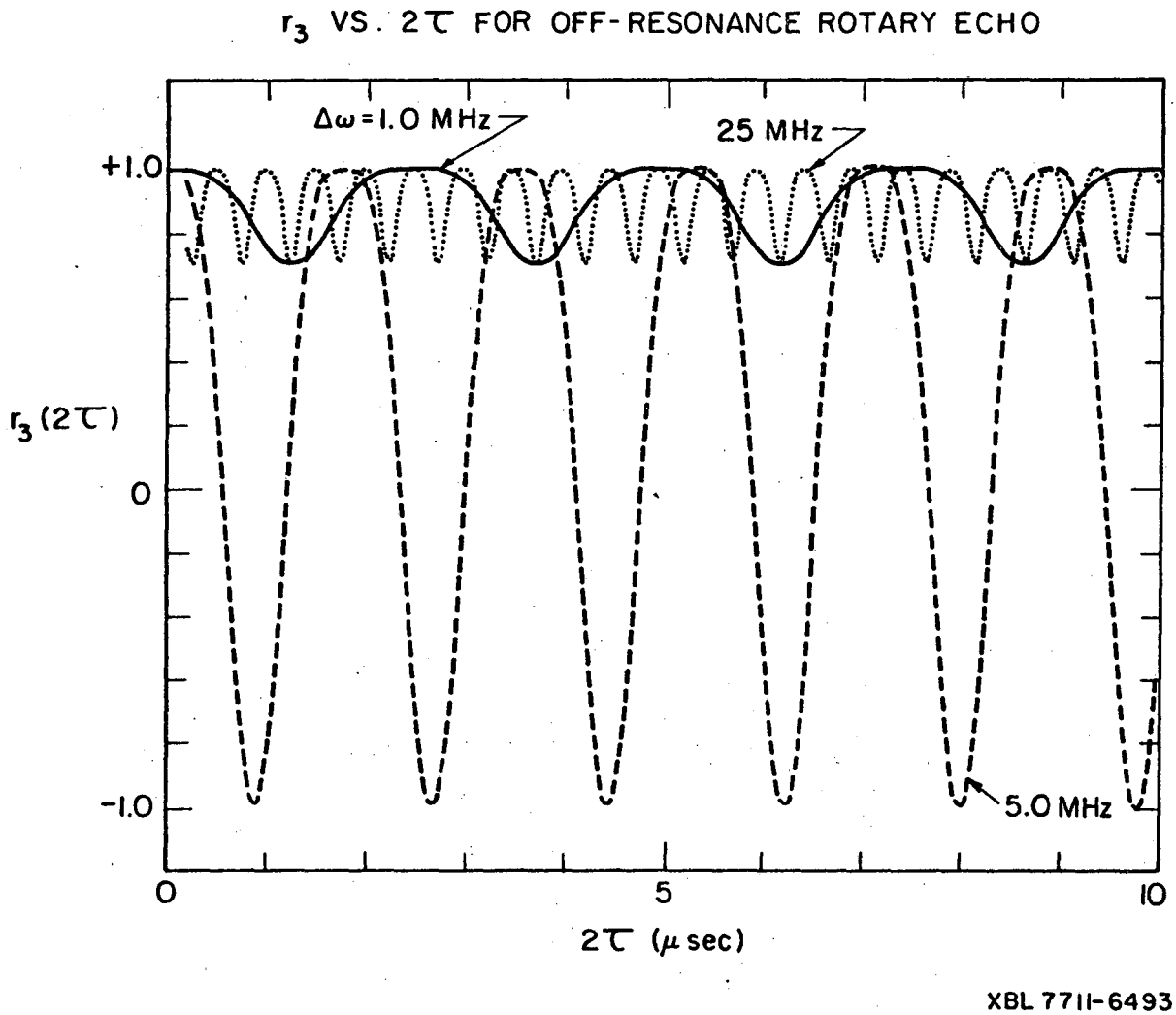
r_3 VS. 2τ FOR OFF-RESONANCE ROTARY ECHO
$\Delta\omega$ = 1.0 MHz
25 MHz
5.0 MHz
+1.0
0
-1.0
$r_3(2\tau)$
0
5
10
2τ (μ sec)
XBL 7711-6493

Figure 6

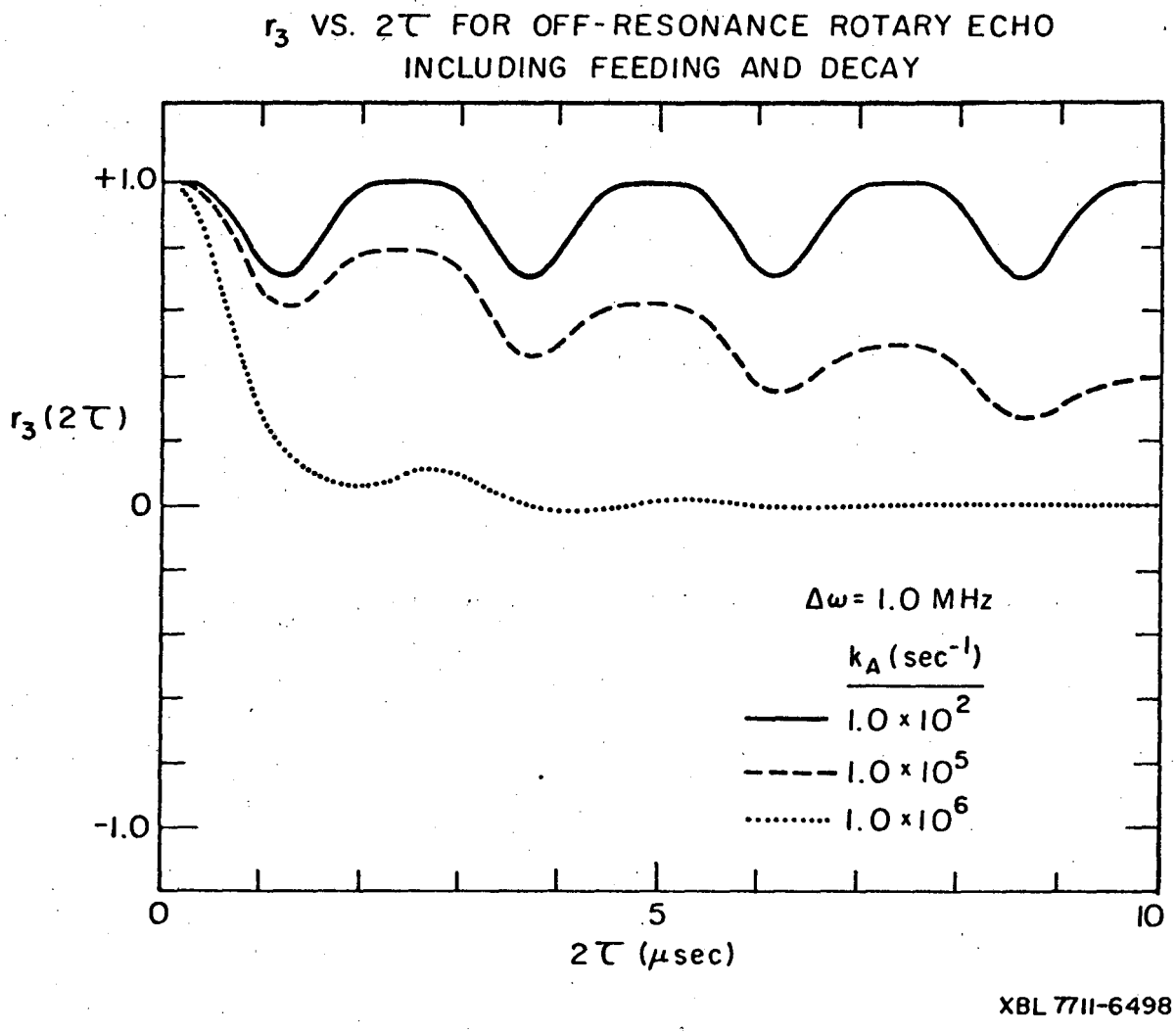
r_3 VS. 2τ FOR OFF-RESONANCE ROTARY ECHO
INCLUDING FEEDING AND DECAY
+1.0
$r_3(2\tau)$
0
-1.0
0
5
10
2τ (μsec)
$\Delta\omega$ = 1.0 MHz
k_A (sec^{-1})
1.0×10^2
1.0×10^5
1.0×10^6
XBL 7711-6498

Figure 7

TECHNICAL INFORMATION DEPARTMENT
LAWRENCE BERKELEY LABORATORY
UNIVERSITY OF CALIFORNIA
BERKELEY, CALIFORNIA 94720